ELSEVIER

Hydrometallurgy 48 (1998) 1–26

hydrometallurgy

The use of on-line off-gas analyses and stoichiometry in the bio-oxidation kinetics of sulphide minerals

M. Boon *, K.Ch.A.M. Luyben, J.J. Heijnen

Kluyver Laboratory of Biotechnology, Department of Biochemical Engineering, Julianalaan 67, 2628 BC Delft, The Netherlands

Received 20 June 1997; revised 30 October 1997; accepted 30 October 1997

Abstract

New theoretical and experimental methods have been developed to examine the chemical and bacterial oxidation kinetics in bio-oxidation of sulphide minerals, which are determined by an 'indirect' mechanism. On-line off-gas analyses to measure the oxygen and carbon dioxide consumption rate in batch and continuous bio-reactors, together with the application of elemental balances, provides a useful method for the accurate and continuous determination of biomass and mineral specific rates, which must form the basis for reliable kinetic equations. The ferric to ferrous iron concentration ratio is a key parameter in the bacterial oxidation of ferrous iron as well as in the chemical oxidation of pyrite. In bio-oxidation experiments with pyrite extremely high $[Fe^{3+}]/[Fe^{2+}]$ ratios were measured using on-line redox potential measurements. Results are illustrated for *Thiobacillus ferrooxidans* in continuous and batch experiments with ferrous iron, and for batch experiments with *Leptospirillum* bacteria with staged addition of pyrite. © 1998 Elsevier Science B.V.

1. Introduction

In recent years there has been a considerable growth in the application of bio-oxidation for the pretreatment of refractory sulphide gold concentrates. Bioleaching is also widely used for copper from low grade ores, and also considerable interest has been shown in the application for sulphidic cobalt, nickel and zinc ores, and the use of bacterial regeneration of ferric iron solution in the in-situ leaching of sulphide minerals.

* Corresponding author. Tel.: +31-15-2781551; fax: +31-15-2782355; e-mail: m.boon@stm.tudelft.nl.

PII S0304-386X(97)00074-1

In a recent study new experimental methods have been developed and applied to determine the rate determining steps in the bio-oxidation of pyrite [1]. It has been shown that pyrite oxidation with *L. ferrooxidans* is determined by two independent sub-processes: (i) The chemical oxidation of the sulphide mineral with ferric iron to ferrous iron and sulphate, (ii) the bacterial oxidation of ferrous iron with oxygen, regenerating ferric iron. This is referred to as the 'indirect' mechanism. From using the kinetic data reported by other authors it was shown from the comparison of (sterile) chemical and bacterial oxidation rates of pyrite at similar conditions, that the bio-oxidation rate of pyrite is a factor of 10 to 20 times faster than the chemical rate [2–4]. These high rates in the presence of bacteria are due to the favourable chemical conditions (i.e., high ferric to ferrous iron ratios) maintained by the bacteria [1,5]. Accordingly, the chemical oxidation of sulphide minerals with ferric iron and the bacterial oxidation of ferrous iron are relevant sub-processes in the bio-oxidation of sulphide minerals. This paper presents the theoretical background of the new experimental techniques that were developed to examine the bacterial and chemical oxidation kinetics of sulphide minerals in bio-oxidation processes.

Most chemical and bacterial oxidation experiments with sulphide minerals have been carried out batch-wise using off-line analyses of the metal ion concentration to determine the oxidation rate of the mineral.

The biomass concentration is usually determined off-line, using cell counts [6–15], organic nitrogen [16,24], protein analyses [17–23], or TOC analyses (total organic carbon) [19,24–26]. Most authors who examined the bacterial ferrous iron oxidation kinetics in batch [27–31] or continuous [29,30,32–35] cultures, only used off-line measurement of the biomass and ferrous iron concentration. More accurate on-line measurement of oxygen and carbon dioxide in the gas-phase, which leads to direct information on O_2 and CO_2 consumption, is often applied in other fields of biotechnology. The oxygen and carbon dioxide consumption rates, r_{O_2} and r_{CO_2} (mol/l/h), in the slurry are known on-line, and, from using elemental and charge balances, also the biomass (C_x), substrate ($[Fe^{2+}]$ or $[FeS_2]$), and product ($[Fe^{3+}]$) concentration can be calculated on line. From this set of data the biomass and mineral specific rates (mol/C-mol/h and mol/mol FeS_2/h, respectively), which are needed in kinetic equations, are known on-line. In this paper it will be shown that in several cases the on-line measurement of the oxygen and carbon dioxide consumption from the gas-phase is sufficient to accurately measure the bio-oxidation kinetics of ferrous iron and mineral sulphides. Another very useful tool is the determination of very low ferrous iron concentrations in the slurry from on-line redox potential measurements in the solution.

The use of these experimental techniques give a significant increase of our understanding of bio-oxidation processes: (i) The mechanism in the bio-oxidation of pyrite with *L. ferrooxidans* has been determined (i.e., the *indirect* mechanism). (ii) A mechanistic kinetic model has been developed for the oxidation of pyrite with *L. ferrooxidans*. (iii) A kinetic model has been developed for the (sterile) chemical oxidation of pyrite with ferric iron. (iv) Accurate kinetic models have been developed for ferrous iron oxidation with *T. ferrooxidans* and with *L. ferrooxidans*. Furthermore, it has been shown that: (v) Dynamic behaviour of *T. ferrooxidans* on ferrous iron can be important in kinetic measurements, and that several measurement methods to determine

the ferrous iron oxidation kinetics (e.g., the effect of the iron concentration, pH, toxic metal ions) are inappropriate. (vi) The bio-oxidation of zinc sulphide with *T. ferrooxidans* is determined by an *indirect* mechanism in which elemental sulphur is produced. (vii) The simultaneous oxidation of ferrous and elemental sulphur by *T. ferrooxidans* are coupled processes, and therefore, the ferrous iron oxidation kinetics of *T. ferrooxidans* is largely effected when elemental sulphur (produced in the chemical oxidation of zinc sulphide) is present. (viii) An experimental technique to measure the chemical oxidation kinetics of sulphide minerals at moderate temperatures (20–35°C) and pH (1.5–2.5), at high ferric to ferrous iron concentrations, using batch cultures with *L. ferrooxidans*, is proposed. (ix) It is suggested how these techniques can be useful in examining bio-oxidation processes for a particular mineral source and bacterial strain. [1,5,36,37].

The use of on-line off-gas analyses and the application of stoichiometry (elemental and charge balances) is here illustrated for three examples of kinetic measurements. (1) Continuous cultures with *T. ferrooxidans* on ferrous iron. (2) Batch cultures with *T. ferrooxidans* on ferrous iron. (3) Batch cultures with *L. ferrooxidans* on pyrite.

2. Theory

2.1. Elemental and charge balances

Autotrophic bacteria, such as *T. ferrooxidans* and *L. ferrooxidans*, use carbon dioxide as their sole carbon source to produce organic matter. A stoichiometric equation for bacterial growth on ferrous iron can be derived from the elemental balances on C, H, O, N, Fe, and the charge balance [38]. Introduction of Y_{sx} as the biomass yield on ferrous iron, and assuming that the biomass composition [38] is represented by $CH_{1.8}O_{0.5}N_{0.2}$, results in the following stoichiometric equation for the bacterial oxidation of ferrous iron,

$$CO_2 + 0.2NH_4^+ + \frac{(1-4.2Y_{sx})}{4Y_{sx}}O_2 + \frac{1}{Y_{sx}}Fe^{2+} + \left(\frac{1}{Y_{]sx}} - 0.2\right)H^+ \rightarrow CH_{1.8}O_{0.5}N_{0.2} + \frac{1}{Y_{sx}}Fe^{3+} + \left(\frac{1}{2Y_{sx}} - 0.6\right)H_2O \quad (1)$$

This equation provides the following relations between production and consumption rates of the compounds. In the equations production rates are positive, consumption rates are negative. According to the definition, $1/Y_{sx}$ is the amount of ferrous iron to be oxidized to produce 1 C-mol of biomass. Therefore, the production rate of biomass equals the ferrous iron oxidation rate times the yield of biomass on that substrate,

$$-r_{Fe^{2+}} = \frac{1}{Y_{sx}}r_x \quad (2)$$

Similarly $1/Y_{ox}$ is defined as the amount of oxygen that is to be consumed to produce 1 C-mol of biomass that oxidizes a certain substrate. So, the production rate of biomass equals the oxygen consumption rate times the yield of biomass on oxygen, Y_{ox},

$$-r_{O_2} = \frac{1}{Y_{ox}} r_x \tag{3}$$

Thus, Eq. (1) directly shows that

$$\frac{1}{Y_{ox}} = \frac{1 - 4.2Y_{sx}}{4Y_{sx}} \tag{4}$$

If it is assumed that no iron precipitates (e.g. jarosite) are formed, the oxidation rate of ferrous iron, $r_{Fe^{2+}}$, equals the production rate of ferric iron, $r_{Fe^{3+}}$, according to the *iron balance*,

$$-r_{Fe^{2+}} = r_{Fe^{3+}} \tag{5}$$

The production rate of bacteria, r_x, is equal to the consumption rate of carbon dioxide, r_{CO_2}, according to the *carbon balance*,

$$-r_{CO_2} = r_x \tag{6}$$

Accordingly, the concentration of bacteria is expressed in moles of organic carbon per litre (C-mol/l). The relation between the oxidation rate of ferrous iron and the oxygen and carbon dioxide consumption rates is called the 'degree of reduction balance' [38] and follows from the stoichiometry,

$$-r_{Fe^{2+}} = -4r_{O_2} - 4.2r_{CO_2} \tag{7}$$

This equation shows the effect of using an integrated stoichiometric equation for ferrous iron oxidation and biomass growth (Eq. (1)) compared with using a separate stoichiometric equation for the oxidation of only ferrous iron which would yield that $r_{Fe^{2+}} = 4r_{O_2}$. However, the term $4.2r_{CO_2}$ in Eq. (7) has only a minor effect with regard to oxygen consumption (5%). In this work the biomass composition, $CH_{1.8}O_{0.5}N_{0.2}$, and the nitrogen balance were not checked.

In bio-oxidation experiments with sulphide minerals the mineral oxidation rate is also coupled to the oxygen and carbon dioxide consumption rate. If pyrite is completely oxidized to ferrous iron and sulphate (i.e., no accumulation of intermediates), the degree of reduction balance is

$$-15r_{FeS_2} = -4r_{O_2} - 4.2r_{CO_2} \tag{8}$$

In bio-oxidation experiments in aerated fermenters with ferrous iron or pyrite, the carbon balance is checked from the comparison of the bacterial growth rate, r_x, and carbon dioxide consumption rate, r_{CO_2} (Eq. (6)). If the carbon balance is met, C_x (C-mol/l) is accurately derived from the total amount of carbon dioxide consumed in the culture. In order to examine whether precipitates are formed, the iron balance, Eq. (5), needs to be checked. For pyrite the iron balance, from $-r_{FeS_2} = r_{Fe^{3+}}$, is checked from weighing the residual pyrite at the end of an experiment. If in cultures with ferrous iron the degree of

reduction balance, Eq. (7), applies, the ferrous iron oxidation rate in continuous cultures on ferrous iron, and also the degree of conversion of ferrous iron in batch cultures, can be directly determined from only the on-line measured oxygen and carbon dioxide consumption. The same holds for pyrite cultures. It is important to recognize that Eq. (8) is only applicable to determine the pyrite oxidation rate, r_{FeS_2}, and the pyrite concentration, $[FeS_2]$, if no accumulation of intermediate products occurs (e.g. in the bio-oxidation of zinc sulphide with *T. ferrooxidans* transient accumulation of ferrous iron and elemental sulphur occurred [37]).

2.2. Specific rates

Rate equations for the bacterial oxidation kinetics are usually expressed in terms of the biomass specific rates (mol/C-mol/h). The biomass specific oxidation (or consumption) rate of compound i, q_i, is defined as the rate per C-mol of biomass,

$$q_i = \frac{|r_i|}{C_x} \tag{9}$$

Accordingly, the biomass specific oxygen consumption rate, q_{O_2}, is defined as the oxygen consumption rate per C-mol of biomass: $q_{O_2} = -r_{O_2}/C_x$, and the (biomass) specific growth rate, μ, is defined by: $\mu = r_x/C_x$. These biomass specific rates are measures of the activity of the bacteria (mol/C-mol/h). They are used in the rate equations which describe their dependence on the process conditions such as ferrous and ferric iron concentration, pH, temperature, etc.

The pyrite specific rate, ν, is introduced as a measure of the reactivity of the pyrite. These mineral specific rates are equivalent to the first order rate constants that are used elsewhere [4]. Because it is assumed that the pyrite oxidation rate can be described according to a surface reaction, the specific pyrite oxidation rate needs to be expressed in terms of moles consumed or oxidized per square metre of pyrite surface per hour. However, because no technique was available to accurately determine the pyrite surface area in slurries, the specific pyrite oxidation rate is expressed per mole of pyrite (mol/mol FeS_2/h), using $[FeS_2]$ as the pyrite concentration. For pyrite conversions up to 50% this will only cause minor errors [3]. The pyrite specific oxidation rate is therefore defined by

$$\nu_{FeS_2} = \frac{r_{FeS_2}}{[FeS_2]} \tag{10}$$

and the pyrite specific oxygen consumption rate is defined by

$$\nu_{O_2} = \frac{r_{O_2}}{[FeS_2]} \tag{11}$$

Due to the occurrence of a dominant ‘indirect’ mechanism, a very useful application of the degree of reduction balance for pyrite, Eq. (8), is the determination of the specific chemical oxidation rate of pyrite, ν_{FeS_2} in Eq. (10), from only the oxygen and carbon dioxide consumption rate [1,5].

2.3. Yield and maintenance of microbial growth

The Pirt equation is applied to relate the substrate consumption and the bacterial growth and maintenance [39]. The primary process in bacterial oxidation reactions is considered to be the oxidation of substrate (e.g., ferrous iron, sphalerite or pyrite). The maximum growth yield, Y_{sx}^{max} (C-mol/mol), is defined as the maximum amount of biomass that can be produced per mole of substrate. The maintenance coefficient, m_s (mol/C-mol/h), is defined as the amount of substrate that is required per unit of time to maintain one C-mol of bacteria. It is assumed that Y_{sx}^{max} and m_s are constants for a certain bacterial strain growing on a certain substrate. Then, according to the empirical Pirt relationship, the following equation predicts the substrate oxidation rate that is required for both the bacterial growth and the maintenance of bacteria,

$$-r_s = \frac{r_x}{Y_{sx}^{max}} + m_s C_x \tag{12}$$

Using the definitions of the actual yield of biomass on substrate, Y_{sx} (Eq. (2)), and specific growth rate, μ (Eq. (9)), this can be rewritten as

$$\frac{1}{Y_{sx}} = \frac{1}{Y_{sx}^{max}} + \frac{m_s}{\mu} \tag{13}$$

Similarly, introducing the maximum yield of biomass on oxygen, Y_{ox}^{max}, and the maintenance coefficient of biomass on oxygen, m_o, the oxygen consumption rate required for growth and maintenance of the bacteria on a certain substrate according to the Pirt equation is

$$-r_{O_2} = \frac{r_x}{Y_{ox}^{max}} + m_o C_x \tag{14}$$

Using the definition of the actual yield of biomass on oxygen, Y_{ox} in Eq. (3), and that of the specific growth rate this equation is rewritten as

$$\frac{1}{Y_{ox}} = \frac{1}{Y_{ox}^{max}} + \frac{m_o}{\mu} \tag{15}$$

Hence, the actual yield of biomass on substrate, Y_{sx}, and oxygen, Y_{ox}, depends on the specific growth rate, μ.

By means of the degree of reduction balance the maximum yield of bacteria on ferrous iron, Y_{sx}^{max}, is related to its maximum yield on oxygen, Y_{ox}^{max}, as

$$Y_{ox}^{max} = \frac{4Y_{sx}^{max}}{1 - 4.2Y_{sx}^{max}} \tag{16}$$

and the maintenance coefficient of bacteria that grow on ferrous iron, m_s, is related to the amount of oxygen that is used for maintenance, m_O, as

$$m_o = \frac{m_s}{4} \tag{17}$$

In bio-oxidation experiments it always needs to be examined whether the Pirt equation applies. It will be shown that the Pirt equation does not apply in the initial phase of a batch culture, where *T. ferrooxidans* is transferred from a low ferrous iron concentration in a continuous culture to a high ferrous iron concentration in a batch culture (Fig. 11). If the Pirt equation is applicable it has several uses:

(a) The specific growth, oxygen and ferrous iron consumption rates are coupled. Therefore, if one kinetic equation is known (e.g., for q_{O_2}), the other rate equations can be derived from Eq. (12) or Eq. (14).

(b) Some authors [40,41] have used the comparison of yield coefficients on different substrates (e.g., Y_{sx}^{max} of *T. ferrooxidans* on ferrous iron, elemental sulphur, and pyrite) to argue that both ferrous iron and reduced sulphur is consumed by the bacteria in the bio-oxidation pyrite, which according to these authors proved the relevance of a 'direct' mechanism (this argument has been examined elsewhere [1]).

(c) It has been shown that often carbon dioxide limitation occurs in bio-oxidation experiments with sulphide minerals [42]. If the maintenance and maximum yield coefficients of a bacterium on a substrate are known, the Pirt equation (Eq. (12)) is useful in predicting the carbon dioxide consumption rate at a particular oxidation rate. The calculation is used to estimate whether the carbon dioxide mass transfer from the aeration air to the slurry is sufficient.

3. Materials and methods

Continuous cultures with *T. ferrooxidans* on ferrous iron were carried out at dilution rates between 0.01 and 0.09 h^{-1} at a total iron concentration of 0.21 M. Oxygen and carbon dioxide off-gas analyses were applied, and the ferric and ferrous iron concentration were determined off-line with a colorimetric method (see below). The biomass concentration was determined off-line (TOC analyses, see below).

Batch cultures with ferrous iron were inoculated with a relatively large inoculum size (10% v/v). This inoculum was cell suspension taken from the continuous culture with *T. ferrooxidans* on ferrous iron. Accordingly, the initial steady state conditions of the cells are accurately known from the continuous culture measurements (C_x, q_{O_2} and μ). Consequently, the initial biomass concentration in a batch culture, $C_x(0)$, is accurately known (which is necessary when using a relatively large inoculum size). The total iron concentration in the batch experiment is equal to that in the continuous culture. The ferrous and ferric iron concentrations in the batch experiment were determined off-line. The use of on-line off-gas analyses of O_2 and CO_2 enabled examination of the dynamic behaviour of the cells when transferred from a low ferrous iron concentration in the continuous culture to a high $[Fe^{2+}]$ in the batch culture.

A new experimental method (staged pyrite addition to batch cultures) has been developed to examine the kinetics of pyrite oxidation with *Leptospirillum* bacteria. This method is described elsewhere [5].

Continuous and batch culture experiments were carried out in stirred and baffled aerated fermenters with a working volume of 2 l ($H/D = 1$), maintained at 30°C by a

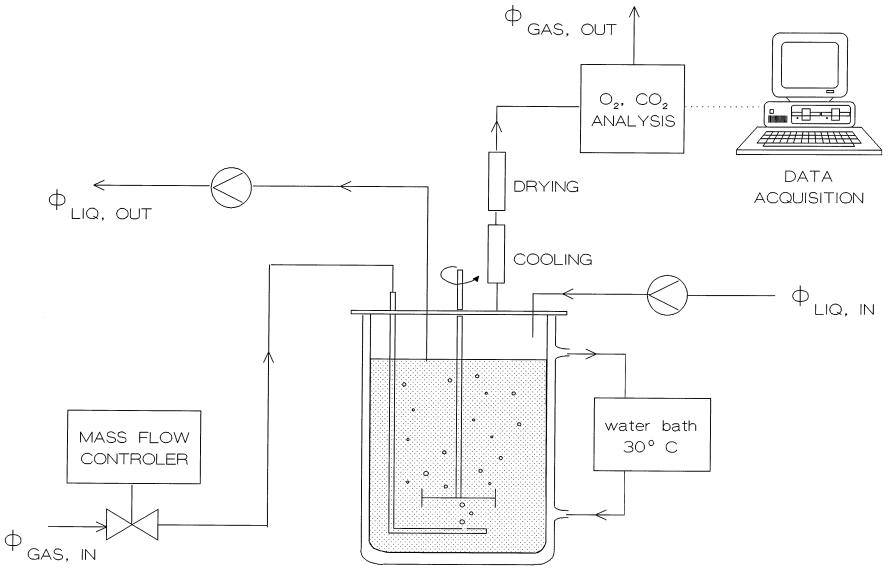

Fig. 1. Fermenter equipment.

water jacket (Fig. 1). In continuous cultures, influent medium flow rate was calculated from the weight decrease of the medium vessel. A servo motor and speed controller were used to agitate the slurry. The aeration flow of dry air was controlled with a Brooks mass-flow controller (model 5850TR and model 5878). The off-gas was dried in a reflux condenser and a Permapure filter. The oxygen concentration in the off-gas and reference air were measured with a Servomex paramagnetic oxygen analyzer (Series 110). The carbon dioxide concentration in the gas phase was measured with a Beckman infrared analyzer (model 864). The oxygen and carbon dioxide concentrations in the off-gas and reference air were monitored on-line using a data acquisition program BIOWATCH [43]. This program also monitored the measurement of the redox potential, and controlled the valves that lead the gas-flows to the analysing apparatus.

The gas–liquid mass transfer of oxygen and carbon dioxide in the fermenter needs to be sufficiently large in order to allow relevant measurements of the bacterial oxidation kinetics, and therefore, the air flow rate and stirring speed need to be high [42]. On the other hand, for accurate measurements a significant decrease of the oxygen and carbon dioxide concentration in the gas phase is needed, which requires a low gas flow rate. The gas–liquid mass transfer coefficients ($k_L a$) in this fermenter were determined at several aeration and stirring rates, using a dynamic measurement (Table 1) [44]. Usually the stirring speed was 400 min^{-1} and the flow rate of air was 12 l/l/h (0.2 vvm). In the example below it is shown that exhaustion of CO_2 in the aeration air easily occurs [42]: At an air flow rate of 12 l/l/h the available amount of carbon dioxide in the gas phase is 1.6×10^{-4} mol CO_2/l/h (3.3×10^{-4} mol CO_2/mol air), which is close to the actually measured values of r_{CO_2} at high growth rates in batch cultures on pyrite (Fig. 15). Therefore, at high growth rates in the culture the air flow rate needs to be larger in

Table 1
Mass transfer coefficients in fermenters used in the experiments

Stirring speed (min^{-1})	Aeration rate (vvm)	$k_L a(O_2)$ (s^{-1})
300	0.1	0.0031
300	0.2	0.0064
600	0.1	0.014
600	0.2	0.027

order to prevent carbon dioxide limitation. Under this restriction the gas–liquid transfer rates are sufficient in the fermenter: assuming that the oxygen and carbon dioxide concentrations in the solution are 50% of the saturation concentration, then the gas–liquid oxygen transfer rate is 3.5×10^{-3} mol/l/h (400 min^{-1}, 12 l/l/h, $k_L a = 0.010$ s^{-1}), and, at 3.3×10^{-4} mol CO_2/mol air, the carbon dioxide transfer rate is 1.5×10^{-4} mol/l/h. In and it can be seen that r_{O_2} and r_{CO_2} are usually below these values.

The solution redox potential was measured with an Ingold combination redox electrode and Metrohm monitor. The electrode consisted of an Ag/AgCl electrode and a platinum reference electrode (type 465). The electrolyte was replaced with 3 M lithium chloride to achieve less precipitate formation at the membrane. In order to determine the ferric to ferrous iron ratio from the measured redox potential, calibration curves were made with samples from the batch or continuous culture. These samples were sterile filtered to remove the cells. Cell suspensions were centrifuged at 5000 min^{-1} for 30 min. Then, the supernatant was filtered with a 0.2 μm membrane filter (Gelman Science) protected with a microfibre filter (Whatman Glass). The sterile media were checked for their zero microbial activity by measurement of the oxygen consumption in a biological oxygen monitor after the addition of ferrous iron solution. The calibration curve was made at 30°C by adding known amounts of ferrous iron. The initial ferrous iron concentration, which is very low, is estimated by extrapolating the curve.

The total organic carbon in samples was measured (off-line) using a Maihak MST2 carbon analysing unit. Total iron and ferrous iron concentrations in cell suspensions were determined (off-line) with the colorimetric *ortho*-phenanthroline method, ASTM D1068. At low ferrous and high ferric iron concentrations the background colour of the ferric iron in the sample causes an error in the colorimetric measurement so, needed to be corrected with the extinction of a blank. Measurements of the ferrous iron concentrations in cell suspensions below 40 mg/l at total iron concentrations above 3 g/l are not accurate because bacteria significantly consume ferrous iron.

A single cell isolate of *T. ferrooxidans* LMD 81.68 (ATCC 19859) was used. The kinetic experiments were performed aseptic but not sterile. Therefore, an immunofluorescence–DNA–fluorescence staining technique [45] was regularly used to check whether *T. ferrooxidans* was still dominant in the cultures.

A wild strain harvested from Gamsberg mine in South Africa was adapted on Prieska pyrite (see below). *Leptospirillum*-like bacteria appeared to be dominant in this culture. These bacteria have the ability to oxidize ferrous iron but not reduced sulphur species (e.g. elemental sulphur, $S_2O_3^{2-}$). With the immunofluorescence method [45] it has been shown that *Thiobacilli* species were insignificant (*T. ferrooxidans* appeared to be unable

to grow on this pyrite source). The *Leptospirillum* culture was regularly checked for the occurrence of *Thiobacillus* species. Besides microscopic examination no further techniques were applied to specify the *Leptospirillum*-like bacteria.

The medium for the bacterial ferrous iron oxidation experiments contained $(NH_4)_2SO_4$ 1 g/l, KCl 0.1 g/l, K_2HPO_4 0.5 g/l, $MgSO_4 \cdot 7H_2O$ 0.2 g/l. Ferrous iron solution was prepared by the addition of $FeSO_4 \cdot 7H_2O > 99.0\%$ (Baker, Holland) to this medium. Medium concentrations in experiments with pyrite were a factor of ten times larger. On-line pH control equipment was not applied in the fermenter because of precipitate formation problems at the pH electrode. The pH in the ferrous iron feed solution was set with 1 M H_2SO_4 such that a pH of about 1.8–1.9 was provided in continuous cultures with *T. ferrooxidans* (note that higher pH in the feed is required at higher dilution rate because less ferrous iron is oxidized). In batch cultures with *T. ferrooxidans* on ferrous iron the pH was manually controlled at pH 1.8–1.9 by the hourly addition of 1 M H_2SO_4. In batch culture experiments with *L. ferrooxidans* on Prieska pyrite the pH was manually controlled at pH 1.5–1.6 by the addition of 4 M NaOH.

A solution of trace elements [46] was added to the culture: 1 ml/l in ferrous iron medium and 10 ml/l in pyrite medium. To prepare a solution of trace elements 15 g/l EDTA is dissolved in demineralized water. Next, 1 g/l $ZnSO_4 \cdot 2H_2O$ is added and the pH is set to 6.0. Then, successively 1.0 g/l $CoCl_2 \cdot 6H_2O$, 1.0 g/l $MnCl_2 \cdot 4H_2O$, 0.5 g/l $CuSO_4 \cdot 5H_2O$, 5.0 g/l $FeSO_4 \cdot 7H_2O$, 0.5 g/l $Na_2MoO_4 \cdot 2H_2O$, and 0.5 g/l $CaCl_2 \cdot 2H_2O$ were added and pH was set to 4.0. This solution contains carbon, for which it needed to be corrected in TOC analyses.

A sieve fraction of 57–75 μm Prieska pyrite (Gamsberg mine, South Africa) that consisted of 90% FeS_2 and 10% quartz was used in bacterial oxidation experiments.

In the measurement of TOC errors up to 10% can occur. In the measurement of $[Fe^{3+}]$ errors up to 5% can occur, while in measuring low $[Fe^{2+}]$ with the colorimetric method errors up to 30% can occur. In Table 2 the percentage errors in the calculation of r_{CO_2} and r_{O_2} from off-gas analyses are given. In continuous cultures low errors are achieved because at least 100 measurement points were available per steady state; lowest errors occur at high dilution rates. In batch cultures each data point is used (per data point 10 measurements in one minute and 20 min between two data points); lowest errors occur at highest O_2 and CO_2 consumption rates. Additionally errors in rates measured in the fermenter are due to errors in the gas flow rate (1%), in the working volume (1%), and in the liquid flow rate (0.1%) (only in continuous cultures).

Table 2
Errors in off-gas analyses

Experiment	Measurement	Range	Error in r_i (mol/l/h)
Continuous culture Fe^{2+}	ΔCO_2	10–100 ppm	1–10%
	ΔO_2	0.04–0.18%	1–5%
Batch culture Fe^{2+}	ΔCO_2	10–100 ppm	3–30%
	ΔO_2	0.04–0.18%	5–25%
Batch culture FeS_2	ΔCO_2	6–200 ppm	1.5–30%
	ΔO_2	0.04–0.40%	2.5–25%

4. Results

4.1. Continuous culture experiments on ferrous iron

As an example, the data processing of continuous culture experiments with *T. ferrooxidans* on ferrous iron is illustrated. The total iron concentration in the feed was 0.21 mol/l and the dilution rates varied between 0.01 and 0.09 h^{-1}. Iron precipitates were formed in several experiments at high dilution rates, which caused a decrease of the total iron concentration up to 10% in the culture. From the comparison of the total iron concentration in the effluent and influent it was known that the precipitation of iron compounds was negligible in the other experiments. Fig. 2 shows the measured ferrous iron concentration, $[Fe^{2+}]$, and the ferrous iron concentration calculated from the degree of reduction balance. Realizing that $r_{Fe^{2+}} = D([Fe^{2+}]_{in} - [Fe^{2+}])$, $[Fe^{2+}]$ is calculated from the following equation:

$$[Fe^{2+}] = [Fe^{2+}]_{in} - \frac{-4r_{O_2} - 4.2r_{CO_2}}{D} \quad (18)$$

At dilution rates larger than $D = 0.08$ the ferrous iron concentrations from Eq. (18) are close to the measured value, whereas at low dilution rates the two values do not agree because then the $[Fe^{2+}]$ in Eq. (18) is the difference between two large numbers in the same range as the errors in the measurements. Above a dilution rate of about 0.07 h^{-1} a significant part of the substrate is not oxidized and the ferrous iron concentration steeply increases. According to kinetic analyses [36] wash-out of biomass would occur at $D = 0.10$ h^{-1} (because the maximum growth rate, $\mu_{max} = 0.10$ h^{-1}), causing that close to this dilution rate the ferrous iron concentration would increase to the influent

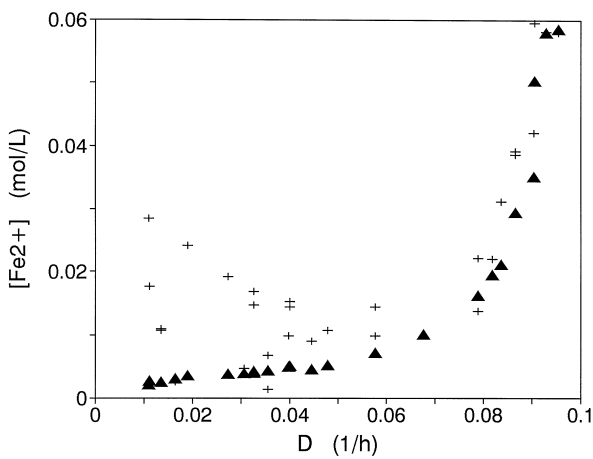

Fig. 2. (▲) Average $[Fe^{2+}]$ (*o*-phenantroline analysis) in a continuous culture with *T. ferrooxidans* at varying steady states and [Fe] = 0.21 mol/l. (+) $[Fe^{2+}]$ calculated from Eq. (18).

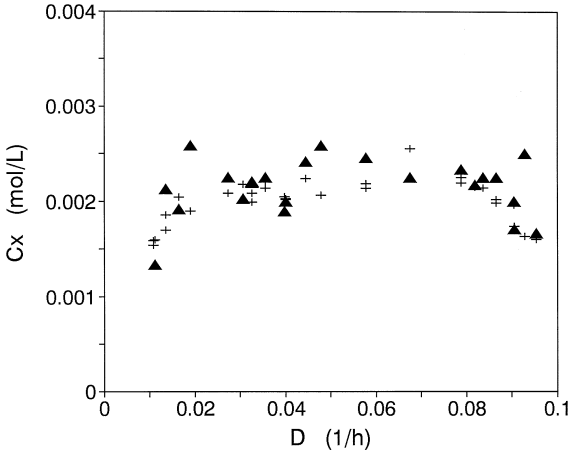

Fig. 3. (▲) C_x measured (TOC) in a continuous culture (same as Fig. 2). (+) C_x from CO_2 consumption.

concentration, $[Fe^{2+}]_{in} = 0.21$ M, while the biomass concentration (Fig. 3) and also the oxygen and carbon dioxide consumption rates (Fig. 4) would decrease to zero. However, no accurate measurements were obtained between $D = 0.085$ and 0.1, due the large effect of the dilution rate on the oxidation rate in this range together with difficulties in the control of the pH in the culture near wash-out (too low pH led to wash-out, too high pH to precipitate formation). Therefore, the highest accurately measured ferrous iron concentration was only 0.06 M (Fig. 2).

In Fig. 3 the biomass concentration in the culture that is derived from TOC analyses is plotted against the dilution rate. The decrease of the biomass concentration at low

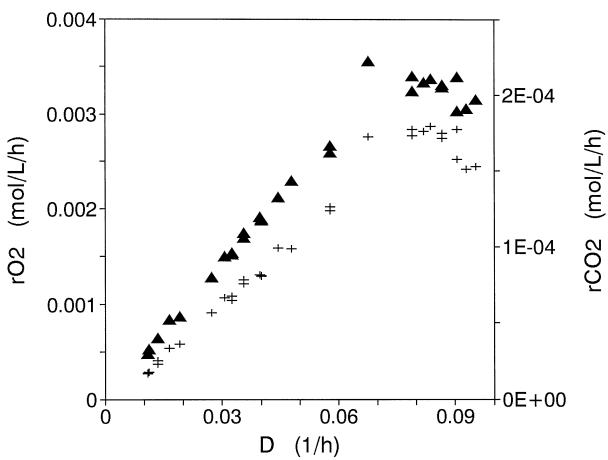

Fig. 4. (▲) r_{O_2} and (+) r_{CO_2} from off-gas analyses in a continuous culture (same as Fig. 2).

dilution rate is due to the increased maintenance requirements of the cells (Eq. (13)). The biomass concentration, C_x (C-mol/l), is also derived from the carbon dioxide consumption rate, r_{CO_2}, and the specific growth rate, μ. In a continuous culture at steady state the specific growth rate of the cells, μ, is equal to the dilution rate, D, and therefore

$$C_x = \frac{-r_{CO_2}}{D} \tag{19}$$

The carbon balance is met because the biomass concentration from TOC and from CO_2 measurements agree (see Fig. 3). Therefore, on-line gas analyses of CO_2 are appropriate to determine the biomass concentration in the continuous culture.

The oxygen consumption rate is derived from the oxygen concentration in the off-gas and reference air,

$$-r_{O_2} = \frac{1}{V_{liq}}\left(\Phi_{gas,in}[O_2]_{ref} - \Phi_{gas,out}[O_2]_{G,out}\right) \tag{20}$$

and the carbon dioxide consumption rate from

$$-r_{CO_2} = \frac{1}{V_{liq}}\left(\Phi_{gas,in}[CO_2]_{ref} - \Phi_{gas,out}[CO_2]_{G,out}\right) \tag{21}$$

It should be noted that, due to the amount of oxygen consumed from the gas phase, $\Phi_{gas,out}$ is not equal to $\Phi_{gas,in}$. Assuming that $\Phi_{gas,out}$ equals $\Phi_{gas,in}$ (because the difference is less than 0.5%), will cause a systematic error of about 20% in the calculation of the oxygen consumption rates. The flow rate of the off-gas, $\Phi_{gas,out}$, is calculated from the N_2 balance in the gas phase,

$$\Phi_{gas,out} = \Phi_{gas,in}\frac{1 - [O_2]_{ref} - [CO_2]_{ref}}{1 - [O_2]_{G,out} - [CO_2]_{G,out}} \tag{22}$$

In this equation the dimensions of the oxygen and carbon dioxide concentration in the gas phase are volume/volume. In Fig. 4 r_{O_2} and r_{CO_2} are plotted against the dilution rate. Each data point shows the average oxygen and carbon dioxide consumption rate that is measured during a steady state. The plot shows the typical behaviour of a continuous culture experiment: The oxygen and carbon dioxide consumption rates increase with the dilution rate because more Fe^{2+} is available per unit of time. Near wash-out the r_{O_2} and r_{CO_2} steeply decrease to zero, because Fe^{2+} is only partly oxidized.

The biomass specific oxygen consumption rate, q_{O_2}, is derived from applying Eq. (9) and plotted against the dilution rate in Fig. 5. The value of q_{O_2} linearly increases with the dilution rate which is in accordance with the Pirt equation.

In Figs. 6 and 7 the reciprocal biomass yield on ferrous iron, $r_{Fe^{2+}}/r_{CO_2}$, and on oxygen, r_{O_2}/r_{CO_2}, are plotted against the reciprocal dilution rate. From these figures it can be seen that the actual yield, Y_{sx}, is dependent on the specific growth rate (D). Eqs. (13) and (15) are applied and yield a straight line with a slope equal to the maintenance coefficients (m_s and m_O, respectively), and with an intercept equal to the reciprocal

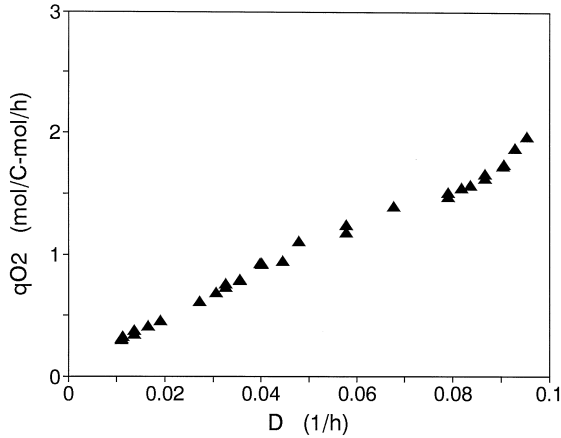

Fig. 5. (▲) q_{O_2} in a continuous culture (same as Fig. 2).

values of the maximum yield ($1/Y_{sx}^{max}$ and $1/Y_{ox}^{max}$, respectively). Accordingly, the Pirt equation applies to continuous cultures of *T. ferrooxidans* on ferrous iron. The fitted values are $Y_{sx}^{max} = 0.012 \pm 0.0005$ mol Fe^{2+}/C-mol, m_s is 0.45 ± 0.10 mol Fe^{2+}/C-mol/h (Fig. 6) and $Y_{ox}^{max} = 0.051 \pm 0.002$ mol O_2/C-mol, m_o is 0.10 ± 0.03 mol O_2/C-mol/h (Fig. 7). From the fitted value of $Y_{sx}^{max} = 0.012 \pm 0.0005$ it follows with Eq. (16) that $Y_{ox}^{max} = 0.051 \pm 0.002$, which is in accordance with the fitted value of Y_{ox}^{max}. Similarly, from the value of $m_s = 0.45 \pm 0.10$ it follows from Eq. (17)) that $m_O = 0.11 \pm 0.025$, which is in accordance with the fitted value of m_o. As discussed already, Eqs. (16) and (17) are applicable because the degree of reduction balance applies.

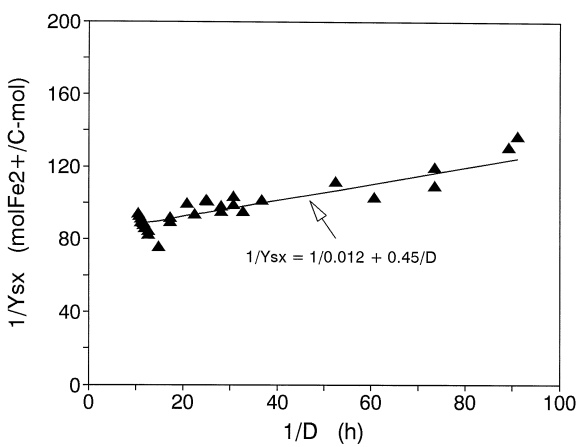

Fig. 6. (▲) Reciprocal yield of *T. ferrooxidans* on ferrous iron against the reciprocal dilution rate in a continuous culture (same as Fig. 2). (————) $1/Y_{sx}$ calculated from Eq. (13) with $Y_{sx}^{max} = 0.012$ mol Fe^{2+}/C-mol and m_s is 0.45 mol Fe^{2+}/C-mol/h.

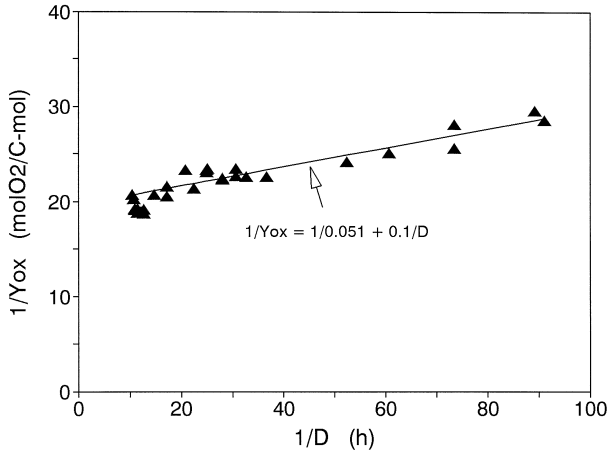

Fig. 7. (▲) Reciprocal yield of *T. ferrooxidans* on oxygen against the reciprocal dilution rate in a continuous culture (same as Fig. 2). (————) $1/Y_{ox}$ calculated with Eq. (15) and $Y_{ox}^{max} = 0.051$ mol O_2 /C-mol and m_o is 0.10 mol O_2 /C-mol/h.

Summarizing, the iron balance, the carbon balance and the degree of reduction balance apply in continuous cultures with *T. ferrooxidans* on ferrous iron. However, the degree of reduction balance is inappropriate to determine low ferrous iron concentrations in the culture and off-line analyses of ferrous iron is needed. On the other hand, the biomass concentration in the culture is accurately determined from the CO_2 analyses in the gas-phase. From these measurements the biomass specific oxygen consumption and growth rate (dilution rate), q_{O_2} and μ, are very accurately related to the ferrous and ferric iron concentration in the culture. This kinetic behaviour has been discussed elsewhere [36]. Because the Pirt equation applies, the growth and oxidation kinetics are related, and therefore, if only one rate equation is known (e.g., q_{O_2}), the other rate equations (e.g., μ and $q_{Fe^{2+}}$) can be immediately derived from using the Pirt equation [36].

4.2. Batch culture experiments on ferrous iron

The second example concerns a batch culture experiment with *T. ferrooxidans* at a total iron concentration of 0.21 mol/l. The inoculum (10% v/v) was taken from a continuous ferrous iron culture in steady state at a dilution rate of 0.033 h^{-1} and a total iron concentration of 0.21 mol/l. The oxygen and carbon dioxide consumption rates (Eqs. (20) and (21)) are plotted in Fig. 8 which shows the typical behaviour of these batch culture experiments: An exponential increase of the oxygen and carbon dioxide consumption rates in the initial phase and a steep drop in the end phase. The surface area under the r_{CO_2} curve is the total amount of CO_2 consumption per litre, and therefore the total amount of biomass, $C_x(t) - C_x(0)$, that is produced at time t is equal to

$$C_x(t) = C_x(0) - \sum_{t_i=0}^{t_{i+1}=t} \frac{r_{CO_2}(t_i) + r_{CO_2}(t_{i+1})}{2}(t_{i+1} - t_i) \qquad (23)$$

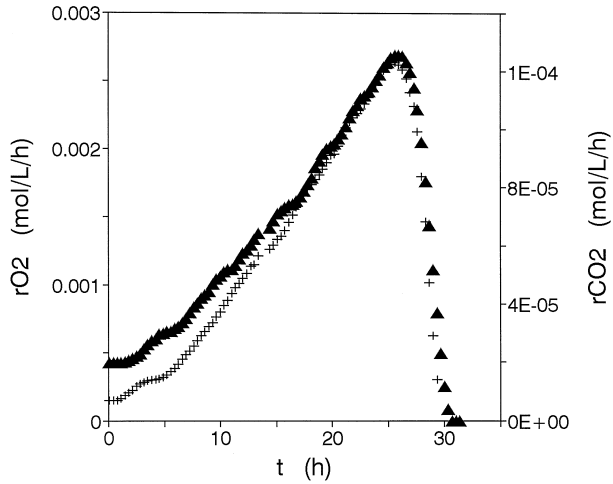

Fig. 8. (▲) r_{O_2} and (+) r_{CO_2} in a batch culture with *T. ferrooxidans* on ferrous iron (0.21 mol Fe/l) derived from on-line off-gas analyses.

In Fig. 9 the biomass concentration determined from the carbon dioxide consumption is plotted (Eq. (23)). TOC was only measured when the experiment was terminated because the amount of sample needed for TOC measurements was too large. In all experiments the measured TOC was equal to the total amount of consumed carbon dioxide, showing a valid carbon balance. The measured ferrous iron concentration and the iron concentration calculated from the total carbon dioxide and oxygen consumption at time t (i.e., the integrated degree of reduction balance which is derived from rewriting

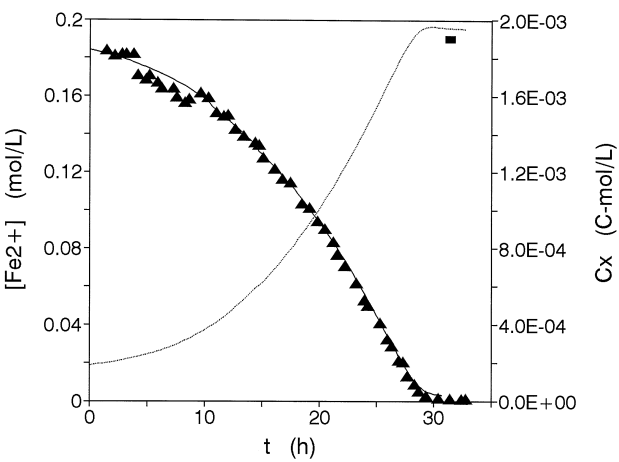

Fig. 9. (· · ·) C_x from the total carbon dioxide consumption in a batch culture (same as Fig. 8). (■) C_x from TOC analyses (only one measurement). (▲) $[Fe^{2+}]$ from *o*-phenantroline analyses. (————) $[Fe^{2+}]$ calculated from degree of reduction balance.

Eq. (7) similar to Eq. (23)) are also plotted in Fig. 9. This plot shows that the measured and calculated ferrous iron concentrations coincide, and therefore, the degree of reduction balance applies. Accordingly, the ferrous iron concentration in a batch culture at time t can be accurately calculated from the oxygen and carbon dioxide consumption at time t. In Fig. 10 both the specific oxygen consumption rate, q_{O_2}, and the specific growth rate, μ, are plotted against time. These specific rates are derived from using the measured oxygen and carbon dioxide consumption rates, $r_{O_2}(t)$ and $r_{CO_2}(t)$ (Fig. 8) and the biomass concentration $C_x(t)$ (Fig. 9). The specific oxygen consumption rate, q_{O_2}, shows the typical behaviour of a batch culture experiment: q_{O_2} is high at high substrate concentration (ferrous iron) and low product concentration (ferric iron which is an inhibitor) in the initial phase, and decreases at decreasing ferrous and increasing ferric concentration in the last phase of the experiment. The specific growth rate, μ, behaves differently because it only slowly increases to μ_{max} which is only reached after 12 h. It appeared that in the initial phase (up to 12 h) the specific growth rate, μ, and the specific oxygen consumption rate, q_{O_2}, are uncoupled. This is clearly seen in Fig. 11, where the reciprocal yield of *T. ferrooxidans* on oxygen, $1/Y_{ox}$, is plotted against the reciprocal specific growth rate, $1/\mu$. The actual yield of biomass on oxygen and substrate in the initial phase of the experiment was very low ($1/Y_{ox}$ is high), and the Pirt equation was only applicable after 12 h. This dynamic behaviour of the cells, and the kinetic behaviour in the batch culture has been extensively discussed elsewhere [36]. The initial phase (< 12 h) was ignored in the determination of the maximum yield and maintenance coefficient on oxygen (Fig. 11) and yielded $Y_{ox}^{max} = 0.0535 \pm 0.002$ C-mol/mol O_2 and $m_O = 0.2 \pm 0.1$ mol O_2/C-mol/h. The maximum yield coefficient of *T. ferrooxidans* on ferrous iron in batch cultures is close to that in continuous cultures, whereas the maintenance coefficient appears to be somewhat larger. However, the errors in m_O determined from these batch culture data are relatively large.

This example of a batch culture clearly shows the usefulness of on-line analyses of O_2 and CO_2 in the gas phase because this method provides accurate biomass and ferrous

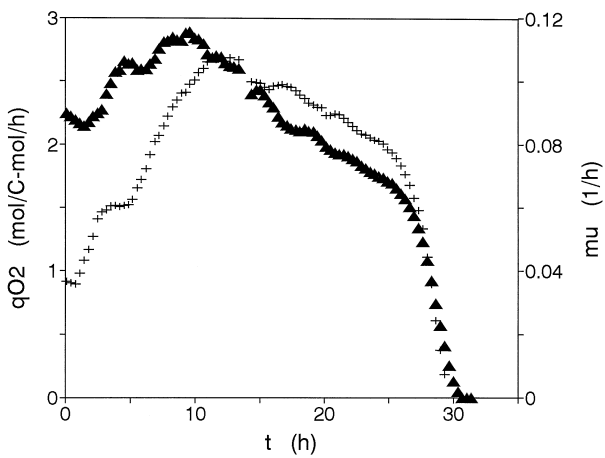

Fig. 10. (▲) q_{O_2} from r_{O_2}/C_x (Fig. 8Fig. 9) and (+) μ from r_{CO_2}/C_x in a batch culture (same as Fig. 8).

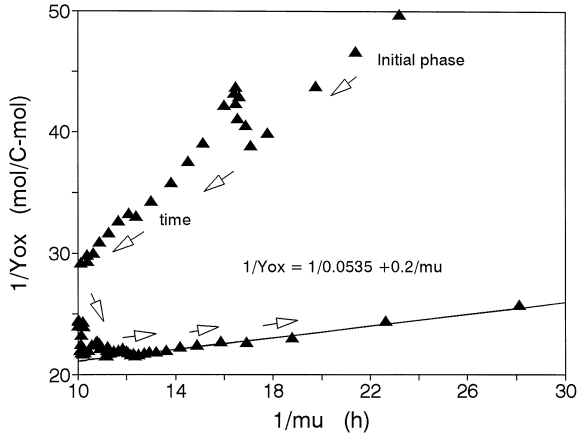

Fig. 11. (▲) $1/Y_{ox}$ $(=r_{O_2}/r_{CO_2})$ against $1/\mu$ in a batch culture (same as Fig. 8). (————) $1/Y_{ox}$ calculated with $Y_{ox}^{max} = 0.0535$ C-mol/mol O_2 and $m_O = 0.2$ mol O_2/C-mol/h.

iron concentrations in the culture, and from these data the biomass specific oxygen consumption and growth rate, q_{O_2} and μ, are accurately known as a function of the ferrous and ferric iron concentration in the culture. These data are sufficient for developing a rate equation for the ferrous iron oxidation kinetics of *T. ferrooxidans* [36]. Another advantage of the use of on-line off-gas analyses is that dynamic behaviour of the cells, as occurred in the initial phase of the batch culture, was discovered.

4.3. Batch culture experiments with staged addition of pyrite

On-line off-gas analyses appeared to be useful in the measurement of step changes in batch experiments. This is illustrated in batch culture experiments with pyrite. Pyrite was bacterially oxidized with *Leptospirillum*-like bacteria. In these experiments pyrite was added step wise to the batch culture. Starting with 2 l of a pyrite grown cell suspension and no pyrite, 4 g of pyrite were added at $t = 23.5$ h, subsequently 6 g at $t = 26.6$ h, 10 g at $t = 28.5$ h, 20 g at 46.4 h, and 20 g at 54.3 h. The amount of pyrite oxidized and the amount of dissolved iron produced (from iron balance: $-r_{FeS_2} = r_{Fe^{x+}}$) in the pyrite batch is calculated from the integrated degree of reduction balance for pyrite (rewriting Eq. (8) similar to Eq. (23)). The calculated pyrite concentration is plotted in Fig. 12, and the calculated total dissolved iron concentration, $[Fe^{x+}]$, is plotted in Fig. 13. The measured total iron concentration (*ortho*-phenantroline method) is plotted in Fig. 13. The values of the calculated and the measured total iron concentration coincided in all the measurements that were carried out. This implies that the degree of reduction balance applies for the pyrite system. Accordingly, because the degree of reduction balance was derived from the assumption that pyrite is completely oxidized to ferric iron and sulphate this stoichiometry is correct (i.e., no intermediate products accumulate in the system). In Fig. 13 also the measured biomass concentration (TOC analyses) and the C_x derived from CO_2 measurements (Eq. (23)), are plotted. The

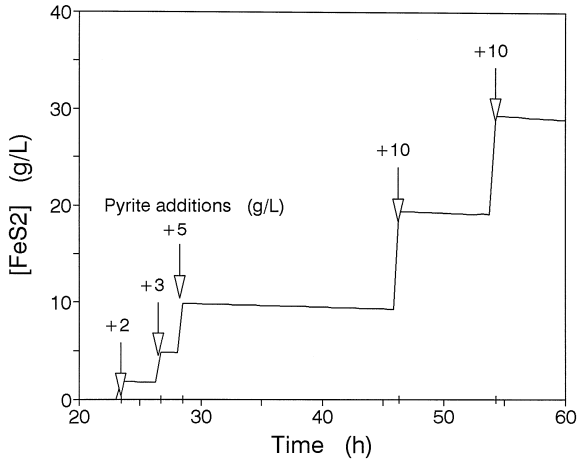

Fig. 12. Staged addition of pyrite in a batch culture with *Leptospirillum*-like bacteria. The arrows show the amount of pyrite added to 2 l of a pyrite grown cell suspension. (————) [FeS_2] derived from the degree of reduction balance.

total biomass concentration from CO_2 measurements and the measured TOC in samples agree, which implies that the biomass concentration is accurately determined from the CO_2 off-gas analyses. No significant difference has been detected between the TOC concentration in samples with and without pyrite. Therefore, the fraction of bacteria attached to pyrite particles is negligible. The step decrease in the total Fe and C_x concentration at 22 h was due to removing 200 ml pyrite-free cell suspension from the culture and replacing it by 200 ml fresh medium.

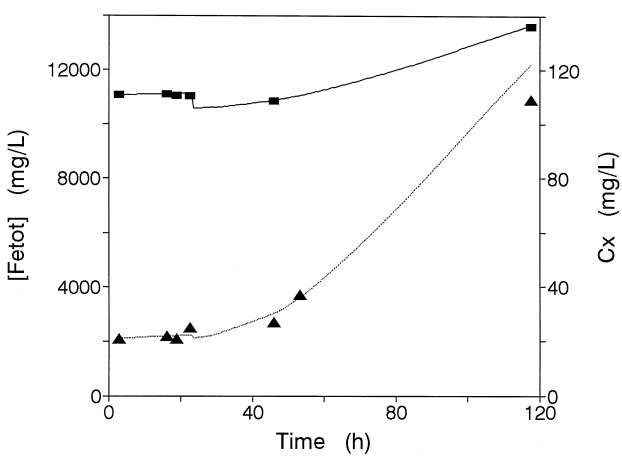

Fig. 13. Staged addition of pyrite in a batch culture with *Leptospirillum*-like bacteria. The arrows show the amount of pyrite added to 2 l of a pyrite grown cell suspension. (————) [FeS_2] derived from the degree of reduction balance.

These measurements show a very important advantage of the on-line off-gas analyses, because the concentrations of biomass, pyrite, and total dissolved iron in batch cultures are accurately and continuously known, which provides a very extensive data set for kinetic evaluation.

The redox potential in the batch culture on pyrite was measured on-line with an $Ag/AgCl//LiCl_3/Pt$ redox meter (Fig. 14). In the initial 22 h this batch culture consisted of a pyrite free cell suspension. In this phase the redox potential is high and the calculated ferrous iron concentration is extremely low ($[Fe^{2+}] = 15 \times 10^{-6}$ M, which is below 1 mg/l). After each pyrite addition the redox potential immediately dropped (implying an increase of the ferrous iron concentration) and then slowly increased again. The lowest redox potential was achieved after the last pyrite addition (highest $[Fe^{2+}] = 150 \times 10^{-6}$ M or 10 mg/l). For comparison: with a standard H_2 redox electrode redox potentials between 950 and 1020 mV would have been measured in this batch culture. The continuous redox potential measurements in pyrite cultures are of major importance in the determination of the bacterial oxidation kinetics of pyrite, which relate both to bacterial Fe^{2+} oxidation and chemical FeS_2 oxidation with Fe^{3+} [1].

In Fig. 15 the oxygen and carbon dioxide consumption rates, r_{O_2} and r_{CO_2}, and their response to pyrite additions are plotted. In the initial 22 h these rates were close to zero because no substrate was available. It was observed that the consumption rates immediately increased after each addition of pyrite, after which the rates slowly increased further. The oxygen and carbon dioxide consumption are stoichiometrically coupled (this is in contrast with the bacterial ferrous iron oxidation where the oxygen and carbon dioxide consumption are uncoupled at the start of a batch culture experiment).

In Fig. 16 the biomass specific oxygen consumption rate and growth rate, q_{O_2} and μ, and their response to pyrite additions, are plotted (Eq. (9)). The biomass specific rates

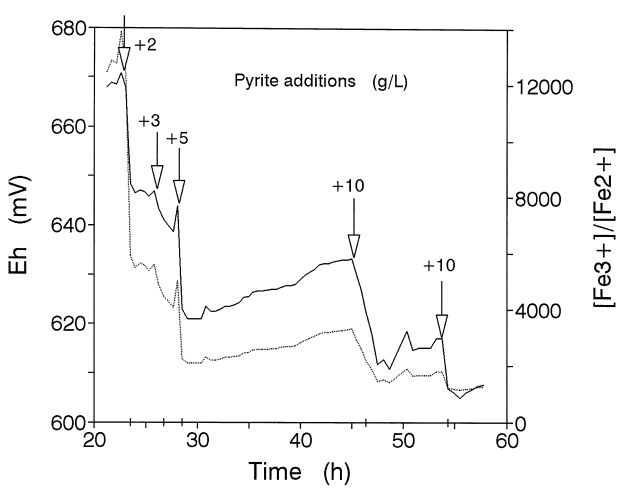

Fig. 14. (————) r_{O_2} and (· · ·) r_{CO_2} pyrite batch culture (same as Fig. 12)

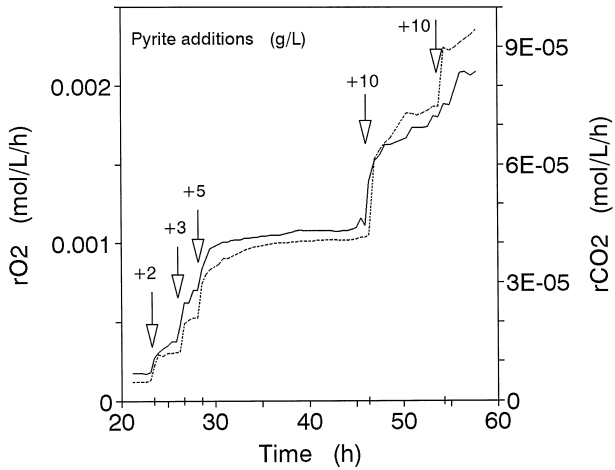

Fig. 15. (————) r_{O_2} and (· · ·) r_{CO_2} pyrite batch culture (same as Fig. 12).

immediately increased after each pyrite addition, and then slowly decreased. The highest biomass specific rate was achieved at the largest pyrite concentration (which is also highest pyrite to biomass ratio). Clearly q_{O_2} increases with $[Fe^{2+}]/[Fe^{3+}]$. In Fig. 17 the pyrite specific oxygen and carbon dioxide consumption rates, ν_{O_2} and ν_{CO_2}, and their response to pyrite additions, are plotted (Eq. (11)). The pyrite specific oxidation rate, ν_{FeS_2} (mol FeS_2/mol FeS_2/h) is easily determined from the degree of reduction balance for pyrite (Eq. (8)). In contrast to the biomass specific rates, the pyrite specific rates decreased after each pyrite addition, and then slowly increased again. Clearly, ν_{FeS_2} decreases with increasing $[Fe^{2+}]/[Fe^{3+}]$.

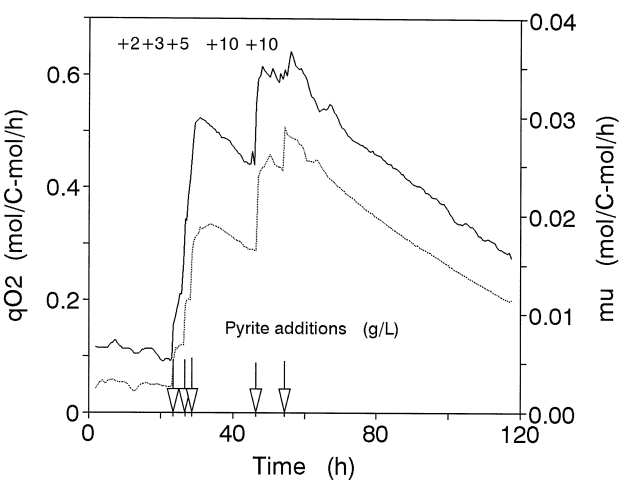

Fig. 16. (————) q_{O_2} and (· · ·) μ in a pyrite batch culture (same as Fig. 12).

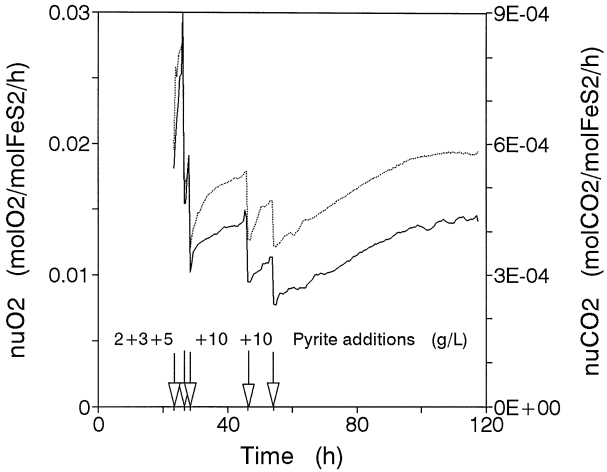

Fig. 17. (————) Pyrite specific oxygen consumption rate (ν_{O_2} written as nuO2), and (· · ·) ν_{CO_2} (written as nuCO2), in a pyrite batch culture (same as Fig. 12).

From these measurements biomass specific rates, q_{O_2} and μ, and pyrite specific rates, ν_{O_2} and ν_{FeS_2}, are known as a function of the ferrous, ferric, pyrite and biomass concentrations in the culture. These data are used in examining the bacterial pyrite oxidation kinetics, which is discussed elsewhere [1].

In Fig. 18 the ratio of the oxygen and carbon dioxide consumption rate, $1/Y_{ox}$, in the batch culture on pyrite is plotted against the reciprocal growth rate, $1/\mu$, and Eq. (15) is applied to derive the maximum yield and maintenance coefficients: $Y_{ox}^{max} = 0.050 \pm 0.002$ mol O_2/C-mol, $m_o = 0.06 \pm 0.025$ mol O_2/C-mol/h. It appears that the maximum

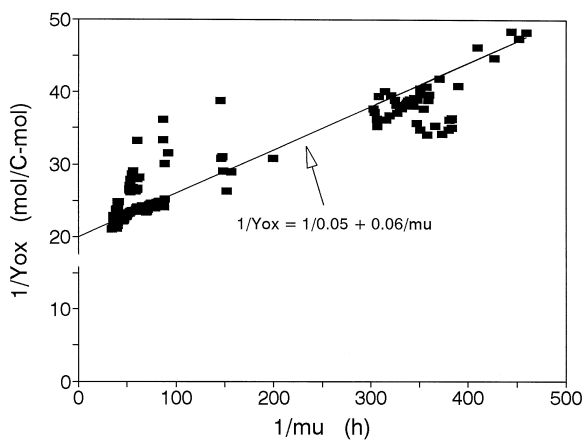

Fig. 18. (■) $1/Y_{ox}$ of *Leptospirillum*-like bacteria on pyrite (same as Fig. 12) against $1/\mu$. (————) $1/Y_{ox}$ calculated (Eq. (15)) with $Y_{ox}^{max} = 0.050$ mol O_2/C-mol, $m_o = 0.06$ mol O_2/C-mol/h.

yield of bacteria on pyrite per mole of oxygen consumed, Y_{ox}^{max} is equal to that on ferrous iron. The maintenance coefficient, m_o, appears somewhat lower. These findings are discussed elsewhere [1].

5. Conclusions

On-line O_2 and CO_2 analyses in the gas phase in batch and continuous cultures, together with the use of stoichiometric equations, has proven to be very useful in examining the bio-oxidation kinetics of ferrous iron and pyrite. The carbon balance was met in all experiments, which showed that the biomass concentrations in continuous and batch cultures were accurately and continuously known from the CO_2 measurement in the gas phase. The iron balance was met in all experiments except when the formation of iron precipitates was visible. The proposed degree of reduction balances, which relate the oxygen and carbon dioxide consumption to the substrate consumption (ferrous iron or pyrite), were applicable (i.e., stoichiometric equation applies and no accumulation of intermediate products occurs). The use of the degree of reduction balance showed that the ferrous iron and pyrite concentrations in batch cultures were accurately and continuously known from only the O_2 and CO_2 measurement in the gas phase; the calculated $[Fe^{2+}]$ was less accurate in continuous cultures compared to off-line iron analyses. On-line off-gas analyses in batch cultures were very useful in determining the occurrence of dynamic growth behaviour of the cells (in ferrous iron cultures), and the response to step changes in the pyrite concentration (batch cultures with staged addition of pyrite). On-line redox potential measurement in batch cultures with pyrite were very accurate in the on-line determination of extremely low ferrous iron concentration and the response of $[Fe^{2+}]$ after a step change in the pyrite concentration. The Pirt equation was applicable to cultures on ferrous iron or pyrite, except for the initial phase of batch cultures on ferrous iron. Consequently, if the kinetic equation for ferrous iron oxidation has been determined, the growth kinetics are also known from applying the Pirt equation [36]. Finally, the methods presented in this work show that a large set of accurate data is obtained from the experiments, which are needed to examine the bacterial ferrous iron or pyrite oxidation, e.g., biomass and pyrite specific rates, q_{O_2}, μ, ν_{O_2}, ν_{FeS_2}, as a function of the concentrations of biomass, pyrite, ferric and ferrous iron [1,36].

6. List of symbols

C_x	Biomass concentration (C-mol/l)
$[CO_2]_{G,in}$	Carbon dioxide concentration in reference air (l/l)
$[CO_2]_{G,out}$	Carbon dioxide concentration in off-gas (l/l)
D	Dilution rate (l/l/h)
E_h	Redox potential in solution (mV)
$[FeS_2]$	Concentration of pyrite (mol/l_{slurry})
$[Fe^{2+}]$	Ferrous iron concentration (mol/l)
$[Fe^{3+}]$	Ferric iron concentration (mol/l)

m_s	Maintenance coefficient on substrate (mol/C-mol/s)
m_O	Maintenance coefficient on O_2 (mol O_2/C-mol/s)
μ	Bacterial specific growth rate (h^{-1})
ν_i	Pyrite specific rate (mol i/mol FeS_2/h)
$[O_2]_{ref}$	Oxygen concentration in reference air (l/l)
$[O_2]_{G,out}$	Oxygen concentration in off-gas (l/l)
Φ_G	Volumetric gas flow rate (m^3/s)
q_i	Bacterial specific rate (mol i/C-mol/s)
r_i	Reaction rate (mol i/l/h)
R	Gas constant (J/mol/K)
t	Time (h)
T	Temperature (K)
V_{liq}	Liquid volume (m^3)
Y_{sx}	Yield of biomass on substrate (e.g.. ferrous iron) (C-mol/mol Fe^{2+})
Y_{ox}	Yield of biomass per mol of oxygen consumed (C-mol/mol O_2)
Y_{sx}^{max}	Maximum yield coefficient on substrate (C-mol/mol Fe^{2+})
Y_{ox}^{max}	Maximum yield coefficient per mole of oxygen (C-mol/mol O_2)

Acknowledgements

C. Ras and D. Reuvers seriously contributed in the experimental part of this work.

References

[1] M. Boon, The mechanism and kinetic model of pyrite (FeS_2) oxidation with *Leptospirillum*-like bacteria, in: Theoretical and Experimental methods in the modelling of bio-oxidation kinetics of sulphide minerals, Ph.D. thesis, TU Delft, The Netherlands, ISBN 90-9009825-9, 1996, pp. 279–344.

[2] M. Boon, J.J. Heijnen, Mechanisms and rate limiting steps in bioleaching of sphalerite, chalcopyrite and pyrite with *Thiobacillus ferrooxidans*, in: A.E. Torma, J.E. Wey, V.L. Lakshmanan (Eds.), Biohydrometallurgical Technologies, vol. 1, The Minerals, Metals and Materials Society, Warrendale, PA, 1993; Proc. Int. Biohydrometallurgy Symp., Jackson, WY, 1993, pp. 217–236.

[3] M. Boon, A literature review of chemical and bacterial oxidation rates of pure sphalerite, chalcopyrite and pyrite, in: Theoretical and experimental methods in the modelling of bio-oxidation kinetics of sulphide minerals, Ph.D. thesis, TU Delft, The Netherlands, ISBN 90-9009825-9, 1996, pp. 23–118.

[4] M. Boon, J.J. Heijnen, Mechanisms and rate limiting steps in bioleaching of sphalerite, chalcopyrite and pyrite with *Thiobacillus ferrooxidans*, in: A.E. Torma, J.E. Wey, V.L. Lakshmanan (Eds.), Biohydrometallurgical Technologies, vol. 1, The Minerals, Metals and Materials Society, Warrendale, PA (1993); Proc. Int. Biohydrometallurgy Symp., Jackson, WY, USA, 1993, pp. 217–236.

[5] M. Boon, J.J. Heijnen, Chemical oxidation kinetics of pyrite in bioleaching processes, Hydrometallurgy submitted for publication.

[6] Y. Konishi, S. Asai, H. Katoh, Bacterial dissolution of pyrite by *Thiobacillus ferrooxidans*, Bioprocess. Eng. 5 (1990) 231–237.

[7] Y. Konishi, H. Kubo, S. Asai, Bioleaching of zinc sulphide concentrate by *Thiobacillus ferrooxidans*, Biotechnol. Bioeng. 39 (1992) 66–74.

[8] T. Yukawa, D. Vanselow, B.J. Ralph, P.L. Rogers, A kinetic model for the bacterial leaching of chalcopyrite ($CuFeS_2$), J. Ferment. Technol. 56 (1) (1978) 45–52.

[9] M. Elzeky, Y.A. Attia, Effects of bacterial adaptation on bioleaching of ferrous sulphides, in: Scheiner, Doyle, Kawatra (Eds.), Biotechnology in Minerals and Metal Processing. AIME, 1989, pp. 139–149.
[10] N.J. Khinvasara, A.D. Agate, Bioreactor leaching of chalcopyrite concentrate from Mosaboni India, in: P.R. Norris, D.P. Kelly (Eds.), Biohydrometallurgy; Proc. Int. Symp. Warwick, 1987, pp. 297–303.
[11] L.B. Sulka, G.R. Chaudhury, R.P. Das, Effect of silver ion on kinetics of biochemical leaching of chalcopyrite concentrate, Trans. Inst. Min. Metall. (Sect C. Min. Process. Extr. Metall.) 99 (1990) C43–46.
[12] R.T. Espejo, P. Ruiz, Growth of free and attached *Thiobacillus ferrooxidans* in ore suspension, Biotechn. Bioeng. 30 (1987) 586–592.
[13] P.R. Norris, D.W. Barr, D. Hinson, Iron and mineral oxidation by acidophilic bacteria: affinities for iron and attachment to pyrite, in: P.R. Norris, D.P. Kelly (Eds.), Biohydrometallurgy; Proc. Int. Symp. Warwick, 1987, pp. 43–59.
[14] G.J. Olson, Rate of pyrite bioleaching by *Thiobacillus ferrooxidans*: Results of interlaboratory comparison, Appl. Environ. Microbiol. March (1991) 642–644.
[15] F. Baldi, T. Clark, S.S. Pollack, G.J. Olson, Leaching of pyrites of various reactivities by *Thiobacillus ferrooxidans*, Appl. Environ. Microbiol. June (1992) 1853–1856.
[16] V. Sanmugasunderam, R.M.R. Branion, D.W. Duncan, A growth model for the continuous microbiological leaching of a zinc sulphide concentrate by *Thiobacillus ferrooxidans*, Biotechn. Bioeng. 27 (1985) 1173–1184.
[17] F. Acevedo, M.A. Cacciuttolo, J.C. Gentina, Comparative performance of stirred and pachuca tanks in the bioleaching of a copper concentrate, in: P.R. Norris, D.P. Kelly (Eds.), Biohydrometallurgy; Proc. Int. Symp. Warwick, 1987, pp. 385–394.
[18] J.G. Kingma, M. Silver, Growth of iron-oxidizing *Thiobacillus* in the presence of chalcopyrite and galena, Appl. Environ. Microbiol. March (1980) 635–641.
[19] P.R. Norris, D.W. Barr, Bacterial oxidation of pyrite in high temperature reactors, in: P.R. Norris, D.P. Kelly (Eds.), Biohydrometallurgy, Proc. Int. Symp. Warwick, 1987, pp. 532–536.
[20] B. Cwalina, L. Weglarz, Z. Dzierzewicz, T. Wilczok, Dependence of effectiveness of leaching of metallic sulphides on enzymes involved in inorganic sulphur metabolism in *Thiobacillus ferrooxidans*, Appl. Microbiol. Biotechnol. 28 (1988) 100–102.
[21] R. Guay, J. Ghosh, A.E. Torma, Kinetics of microbiological production of ferric ion for heap and dump leaching, in: Scheiner, Doyle, Kawatra (Eds.), Biotechnology in Minerals and Metal processing, AIME, 1989, pp. 95–111.
[22] A.H. Basaran, O.H. Tuovinen, Iron pyrite oxidation by *Thiobacillus ferrooxidans*: sulfur intermediates, soluble end products, and changes in biomass, Coal Preparation 5 (1987) 39–55.
[23] Y.C. Chang, A.S. Myerson, Growth models of the continuous bacterial leaching of iron pyrite by *Thiobacillus ferrooxidans*, Biotechn. Bioeng. 24 (1982) 889–902.
[24] L.S. Gormely, D.W. Duncan, R.M.R. Branion, K.L. Pinder, Continuous culture of *Thiobacillus ferrooxidans* on a zinc sulphide concentrate, Biotechnol. Bioeng. 17 (1975) 31–49.
[25] M.A. Blancharte-Zurita, R.M.R. Branion, R.W. Lawrence, Microbiological leaching of chalcopyrite concentrates by *Thiobacillus ferrooxidans*; a comparative study of a conventional process and a catalyzed process, in: P.R. Norris, D.P. Kelly (Eds.), Biohydrometallurgy, Proc. Int. Symp., Warwick, 1987, pp. 273–285.
[26] F.C. Boogerd, M.M.Q. van Alphen, W.J. van Anrooij, J.C. de Bruyn, P. Bos, J.G. Kuenen, The role of growth and maintenance in the oxidation of pyrite in batch culture by a moderately thermophilic, facultative chemolithoautotroph, in: J. Salley, G.L. McCready, P.L. Wichlacz (Eds.), Proc. Int. Symp. Biohydrometallurgy, CANMET, 1989, pp. 735–761.
[27] D.T. Lacey, F. Lawson, Kinetics of the liquid–phase oxidation of acid ferrous sulphate by the bacterium *Thiobacillus ferrooxidans*, Biotechnol. Bioeng. 12 (1970) 29–50.
[28] D.P. Kelly, C.A. Jones, Factors affecting metabolism and ferrous iron oxidation in suspensions and batch cultures of *Thiobacillus ferrooxidans*: relevance to ferric iron leach regeneration, in: L.E. Murr, A.E. Torma, J.A. Brierley (Eds.), Metallurgical Applications of Bacterial Leaching and Related Microbiological Phenomena, Academic Press, New York, 1978, pp. 19–44.
[29] J. Braddock, H.V. Luong, E.J. Brown, Growth kinetics of *Thiobacillus ferrooxidans* isolated from arsenic mine drainage, Appl. Environ. Microbiol. July (1984) 48–55.

[30] M.S. Liu, R.M.R. Branion, D.W. Duncan, The effects of ferrous iron, dissolved oxygen, and inert solids on the growth of *Thiobacillus ferrooxidans*, Can. J. Chem. Eng. 66 (1988) 445–451.
[31] S.R.B. Shrihari, R. Kumar, K.S. Gandhi, Modelling of Fe^{2+} oxidation by *Thiobacillus ferrooxidans*, Appl. Microbiol. Biotechnol. 33 (1990) 524–528.
[32] D.G. MacDonald, R.H. Clark, The oxidation of aqeous ferrous sulphate by *Thiobacillus ferrooxidans*, Can. J. Chem. Eng. 48 (1970) 669–676.
[33] R. Guay, M. Silver, A.E. Torma, Ferrous iron oxidation and uranium extraction by *Thiobacillus ferrooxidans*, Biotechnol. Bioeng. 19 (1977) 727–740.
[34] C.A. Jones, D.P. Kelly, Growth of *Thiobacillus ferrooxidans* on ferrous iron in chemostat culture: influence of product and substrate inhibition, J. Chem. Tech. Biotechnol. 33 B (1983) 241–261.
[35] J.R. Smith, R.G. Luthy, A.C. Middleton, Microbial ferrous iron oxidation in acidic solution, J. Water Pollut. Control Fed. 60 (4) (1988) 518–530.
[36] M. Boon, The kinetic modelling of ferrous iron oxidation with *T. ferrooxidans* and *L. ferrooxidans*, in: Theoretical and experimental methods in the modelling of bio-oxidation kinetics of sulphide minerals, Ph.D. thesis, TU Delft, The Netherlands ISBN 90-9009825-9, 1996, pp. 197–244.
[37] M. Boon, The mechanism of sphalerite (ZnS) oxidation with *T. ferrooxidans*, in: Theoretical and experimental methods in the modelling of bio-oxidation kinetics of sulphide minerals, Ph.D. thesis TU Delft, The Netherlands, ISBN 90-9009825-9, 1996, pp. 244–278.
[38] J.A. Roels, Energetics and Kinetics in Biotechnology, Elsevier Biomedical Press, Amsterdam, 1983.
[39] S.J. Pirt, Maintenance energy: A general model for energy limited and energy sufficient growth, Arch. Microbiol. 133 (1982) 300–302.
[40] G.J.M.W., Arkesteyn, Pyrite oxidation by *Thiobacillus ferrooxidans* with special reference to the sulphur moiety of the mineral, in: Ph.D. thesis: Contribution of microorganisms to the oxidation of pyrite, Wageningen, The Netherlands, 1980, pp. 39–53.
[41] W. Hazeu, D.J. Schmedding, O. Goddijn, P. Bos, J.G. Kuenen, The importance of the sulphur-oxidizing capacity of *Thiobacillus ferrooxidans* during leaching of pyrite, in: O.M. Neysel, R.R. van der Meer, K.Ch.A.M. Luyben (Eds.), Proc. 4th Eur. Congr. Biotechnol., vol. 3, Elsevier, Amsterdam, 1987, pp. 497–499.
[42] M. Boon, J.J. Heijnen, Gas–liquid mass transfer phenomena in bio-oxidation experiments of sulphide minerals: A critical review of literature data, Hydrometallurgy submitted for publication.
[43] C. Hellinga, Manual BIOWATCH 1993, Applicon Dependable Instruments, Schiedam, The Netherlands.
[44] K. van het Riet, Review of measuring methods and results in nonviscous gas–liquid mass transfer in stirred vessels, Ind. Eng. Chem. Process Des. Dev. 18 (3) (1979) 357–364.
[45] G. Muyzer, A. de Bruin, D.J.M. Schmedding, P. Bos, P. Westerbroek, G.J. Kuenen, A combined immunofluorescence–DNA–fluorescence staining technique for enumeration of *Thiobacillus ferrooxidans* in a population of acidophilic bacteria, Appl. Environ. Microbiol. April (1987) 660–664.
[46] W. Vishniac, M. Santer, The thiobacilli, Bact. Rev. 21 (1957) 195–213.